Available online at www.sciencedirect.com
ScienceDirect
Polymer 48 (2007) 6457–6463
polymer
www.elsevier.com/locate/polymer

Electronic structure and optical properties of germanium-bridged platinum(II)-containing diethynylfluorene monomer and oligomers: A theoretical investigation

Li Yang [a], Ji-Kang Feng [a,b,*], Wai-Yeung Wong [c,**], Suk-Yue Poon [c]

[a] State Key Laboratory of Theoretical and Computational Chemistry, Institute of Theoretical Chemistry, Jilin University, Changchun 130023, People's Republic of China
[b] Department of Chemistry, Jilin University, Changchun 130023, People's Republic of China
[c] Department of Chemistry and Centre for Advanced Luminescence Materials, Hong Kong Baptist University, Waterloo Road, Hong Kong, People's Republic of China

Received 23 April 2007; received in revised form 18 June 2007; accepted 19 June 2007
Available online 28 June 2007

Abstract

We apply quantum-chemical techniques to investigate the structural, electronic, and optical properties of some platinum-containing fluorenyleneethynylenegermylene-derived monomers and oligomers. The aim of our quantum-chemical calculations is to investigate the role of the transition metal centers in the organometallic system in terms of electronic structure and to estimate the influence of metal on the optical properties of the monomer and oligomers. The results indicate that there is a weak electronic interaction between the metal-based fragment and the π-conjugated organic segments, and consequently the photophysical properties are mainly based on the fluorenyleneethynylene (TFT) π-conjugated fragment with little contribution from the metal center. The role of metal center can be described as weak delocalization coupled with strong localization characteristic along the organometallic backbone. The introduction of platinum ions into the π-conjugated structure leads to bathochromic shifts in the absorption features as compared to those for the free ligands.

Keywords: Platinum; Germanium-bridged; Oligomers

1. Introduction

Conjugated organometallic systems represent an interesting and active area of research in the materials industry because of their potential applications in optoelectronic devices, such as light-emitting diodes (LEDs) [1], lasers [2], and photocells [3]. One of the most promising systems is represented by the rigid-rod polyyne complexes and polymers of the type *trans*-$[Pt(PBu_3)_2-C\equiv C-R-C\equiv C-]_n$ (R = phenyl, pyridyl, alkynyl, oligothienyl, fluorene, etc.) [4] where the optical and electronic properties of the materials can be adjusted by varying the spacer units. One of the merits in the present system is that incorporation of a heavy platinum center in the polymer chain induces strong spin–orbit coupling to allow light emission from the triplet excited state of the conjugated ligand and higher quantum efficiencies may be achieved in the light-emitting devices by harvesting the energy of the non-emissive triplet excitons [5].

On the other hand, organosilicon polymers are becoming important in many aspects of device technology since they can act as functional materials such as semiconductors, hole-transporting and heat-resistant materials and ceramic precursors. In light of the findings in some conjugated polymers (e.g. poly(fluorenes)) [6] that the light-emitting performance can be improved by the deliberate inclusion of conjugation-

* Corresponding author. Department of Chemistry, Jilin University, Changchun 130023, People's Republic of China. Tel.: +86 431 8499592; fax: +86 431 8945942.
** Corresponding author. Tel.: +86 852 34117074; fax: +86 852 34117348.
E-mail addresses: jikangf@yahoo.com (J.-K. Feng), rwywong@hkbu.edu.hk (W.-Y. Wong).

0032-3861/$ - see front matter © 2007 Published by Elsevier Ltd.
doi:10.1016/j.polymer.2007.06.058

interrupting units and introduction of disorder to the conjugated system, the sp^3 silicon unit is introduced as a good spacer group in metal polyynes, which can also efficiently depress chain aggregation and increase quantum efficiency. However, little is understood about related systems with the heavier group 14 element germanium. Recently, Wong et al. [7] reported the unprecedented synthesis and photophysics of stable blue-light-emitting oligomers of (fluorenyleneethynylenegermylene)s with alternating Ge and diethynylfluorene units. These spectroscopic and structural features are a big challenge to the interplay between theory and experiment and have important implications for the spectroscopy and photochemistry of the broad and important class of rigid-rod transition metal polymers containing conjugation-interrupting sp^3-Ge linker. Moreover, their photochemistry and photophysics represent a challenge to the understanding of excited-state dynamics.

In contrast to the overwhelming experimental studies, so far there are only a few theoretical investigations on the type of rigid-rod transition metal polymers, in spite of the fact that theoretical methods can be extremely useful to better understand the nature of both the ground and the excited states. For commercial exploitation of these materials and for direct application-aimed synthesis, a thorough understanding of the structure–property relationship is necessary. In this paper, the first examples of Ge-bridged Pt(II) metallooligomers and polymers $(Pt–Ge–TFT)_n$ $(n = 1–3)$ as well as their free ligand precursors $(Ge–TFT)_n$ $(n = 1–3)$ (see Fig. 1) are investigated employing density functional theory (DFT) and time-dependent DFT (TDDFT) calculations. We performed quantum-chemical studies pursuing a three-fold objective: (i) the determination of the structural features and the nature of the bonding between the metal center and diethynylfluorene, (ii) the understanding of the role of sp^3-Ge linker in limiting the effective conjugation length (ELC), (iii) the exploration of the role of the transition metal center in the organometallic system in terms of electronic structure and the estimation of the influence of metal on the optical properties of the Pt polyyne polymers.

2. Computational details

Ground-state electronic structure calculations on all oligomers studied in this work have been performed with the density functional theory (DFT) on the SGI origin 2000 server employing Gaussian 03 program package [8]. The functional used throughout this study is the B3LYP, consisting of non-local hybrid exchange functional as defined by Becke's three-parameter equation and the non-local Lee–Yang–Parr correlation functional. Since it is very difficult to use high-level basis sets to treat these systems with the growing molecular size from monomer to oligomers, the second and the third row elements (H, C, P) were described with the split valence 6-31G* basis set of atomic orbitals, while on the germanium atoms we used the 6-31+G* basis set containing a diffuse sp shell, due to the highly polarizable nature of this atom. Owing to the large number of electrons and to account for relativistic effects, basis sets with inner electrons substituted by effective core potentials (ECP) were employed for Pt. In this paper, platinum has been described using ECP60MWB pseudopotential of the Stuttgart/Bonn group (where M indicates that the neutral atom is used in the derivation of the ECP and WB implies the use of the quasirelativistic approach described by Wood and Boring). This yields ECP60MWB(8s7p6d)/[(6s5p3d)]//6-31+G*(Ge)/6-31G*(H,C,P)

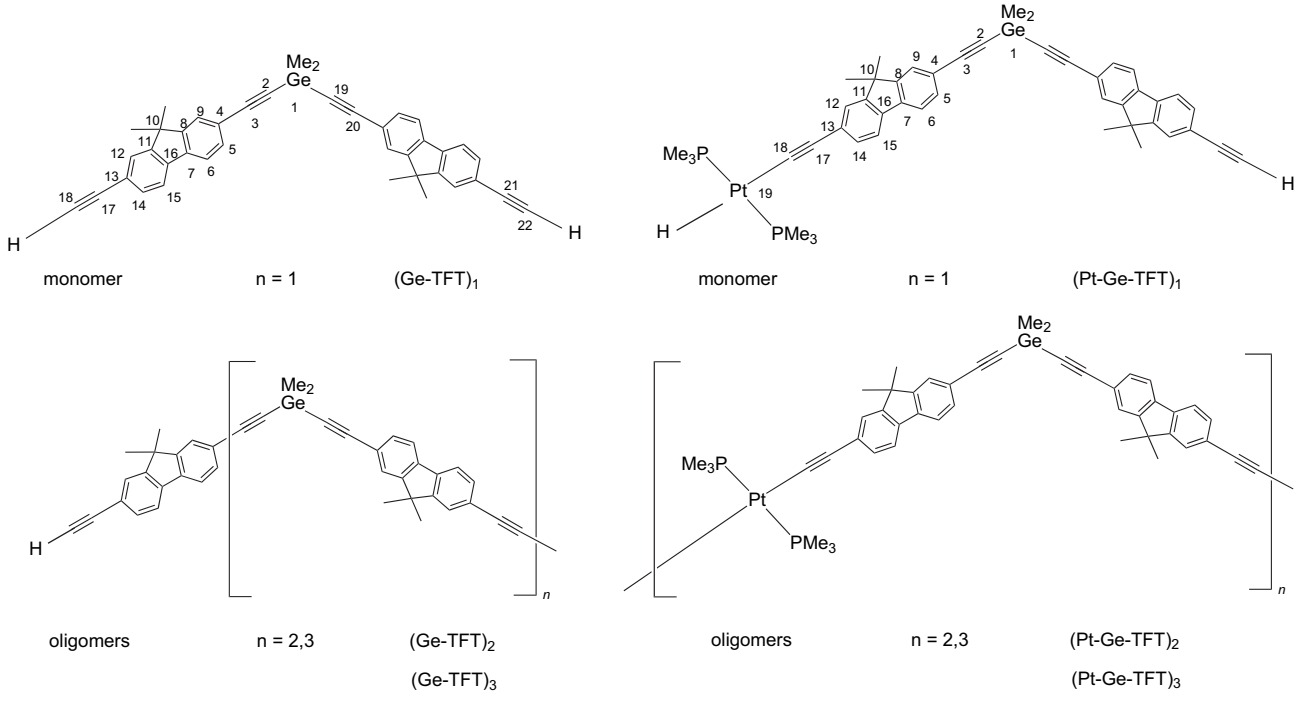

Fig. 1. Structures of the monomer and oligomers investigated in this study: $(Ge–TFT)_n$ $(n = 1–3)$ and $(Pt–Ge–TFT)_n$ $(n = 1–3)$.

basis set for $(Ge-TFT)_n$ ($n = 1-3$) and $(Pt-Ge-TFT)_n$ ($n = 1-3$) systems, respectively, denoted as E60.

The TDDFT, which has been used to study systems of increasing complexity due to its relatively low computational cost and also to include in its formalism the electron correlation effects, is also employed to calculate the vertical electronic excitation spectra [9]. Furthermore, applications of TDDFT approaches have recently been reported on transition metal complexes which gave a considerably good result [10]. Transition energies will be calculated at the ground-state and excited-state geometries by TDDFT at B3LYP level.

3. Results and discussion

3.1. Ground-state structures

In Fig. 1 the molecular structures of the investigated monomer and oligomers $(Ge-TFT)_n$ ($n = 1-3$) and $(Pt-Ge-TFT)_n$ ($n = 1-3$) are shown. The triple bonds are abbreviated by T and the dimethylfluorene ring is denoted as F. It should be pointed out that the dihexyl substitution at C-9 in the fluorene ring, which can improve the solubility and processability of polymers without significantly increasing the steric interactions in the polymer backbone, was replaced by dimethyl groups for the sake of reducing the time of calculation. In fact, it has been proved that the presence of alkyl groups at 9-positions does not significantly affect the equilibrium geometries and thus the electronic and optical properties [11].

The selected pertinent bond lengths and angles of $(Ge-TFT)_1$ optimized by B3LYP/E60 DFT calculations are compared with crystallographic data and summarized in Table 1. Meanwhile, the structural parameters for $(Pt-Ge-TFT)_1$ by B3LYP/E60 are also listed in Table 1 for the sake of comparison of the structure variation upon the introduction of platinum metal. The optimized isocontours of $(Ge-TFT)_1$ and $(Pt-Ge-TFT)_1$ are also appended to Table 1. The differences of bond lengths and angles between calculated and experimental structures are within 0.08 Å and 3° as shown in Table 1. In spite of the discrepancies, the calculated results can still reflect the significant trend, for example the C≡C bond lengths closer to the Ge atom are longer than those farther away.

In general, the platinum Ge-linked diethynylfluorene monomer and its free ligand have similar structural characters as depicted (Fig. 2). To our knowledge, this is the first structurally characterized example of a Ge-bridged Pt(II) metallopolymer. There are two structurally independent but similar molecules per asymmetric unit with the −C≡C−(9,9-dimethylfluorene)−C≡C− units alternately connected by the $GeMe_2$ unit in a linear fashion. The linearity of the acetylene units is evident from the bond angles of Ge−C(sp)−C(sp) with the average value of 179°. The C≡C bond lengths lying around 1.219 Å are typical of metal−acetylide σ bonding and the C≡CH bond shows a slight shortening of bond length (1.210 Å) due to the libration effect. The sp^3-hybridized Ge atom was shown to adopt a tetrahedral geometry, which limits the conjugation length.

In the case of $(Pt-Ge-TFT)_1$, the coordination geometry at the Pt center is square-planar and the two PMe_3 groups are positioned *trans* to each other and the capping groups are connected by the Ge linker. From Table 1, we can still detect the structural variation by the introduction of Pt metal. The Ge−C(sp) single bond lengths are equal (1.896 Å) in $(Ge-TFT)_1$, but are different (1.909 and 1.914 Å, respectively) in $(Pt-Ge-TFT)_1$ in the presence of Pt metal. In addition, the C≡C bond length closest to Pt lengthens by about 0.02 Å.

Table 2 presents the variation of calculated bond length with the number of repeating units *n* in the series of oligomers

Table 1
Comparison of calculated and experimental structural data for $(Ge-TFT)_1$ and the calculated parameters for $(Pt-Ge-TFT)_1$ (bond length: Å; bond angles: deg)

	Ge−C(2)	Ge−C(19)	C(2)−C(3)	C(17)−C(18)	C(19)−C(20)	C(21)−C(22)	Pt−C(18)	Ge−C(2)−C(3)	Ge−C(19)−C(20)
Calc[a]	1.896	1.896	1.219	1.210	1.219	1.210		179.15	179.17
Expt[b]	1.90(1)	1.87(1)	1.20(2)	1.16(2)	1.21(2)	1.13(2)		175.6(8)	176.(1)
Calc[c]	1.909	1.914	1.220	1.231	1.219	1.211	2.059	178.94	178.87

[a] The optimized parameters for $(Ge-TFT)_1$ by B3LYP/E60.
[b] The experimental parameters for $(Ge-TFT)_1$ in Ref. [7].
[c] The optimized structure for $(Pt-Ge-TFT)_1$ by B3LYP/E60.

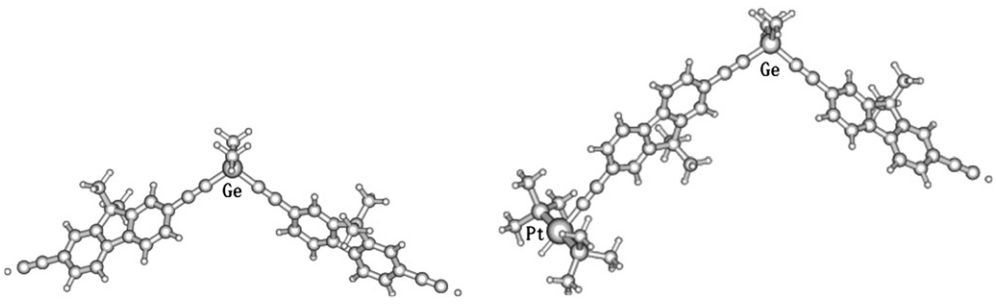

Fig. 2. The optimized structures of $(Ge-TFT)_1$ (left) and $(Pt-Ge-TFT)_1$ (right) calculated by B3LYP/E60.

Table 2
Selected optimized bond lengths (Å) of $(Ge-TFT)_n$ and $(Pt-Ge-TFT)_n$ ($n = 1-3$) calculated by B3LYP/E60

	$(Ge-TFT)_1$	$(Ge-TFT)_2$	$(Ge-TFT)_3$	$(Pt-Ge-TFT)_1$	$(Pt-Ge-TFT)_2$	$(Pt-Ge-TFT)_3$
Ge(1)–C(2)	1.896	1.900	1.896	1.909	1.910	1.911
C(2)≡C(3)	1.219	1.220	1.219	1.220	1.220	1.220
C(3)–C(4)	1.426	1.426	1.426	1.426	1.426	1.426
C(13)–C(17)	1.429	1.430	1.429	1.427	1.428	1.427
C(17)≡C(18)	1.210	1.210	1.211	1.231	1.230	1.229
Pt–C≡C				2.059	2.023	2.014
Pt–H				1.631	1.632	1.631

$(Pt-Ge-TFT)_n$ and their conjugated segments $(Ge-TFT)_n$ ($n = 1-3$), because the bond angles and dihedrals do not suffer appreciable variation with the oligomer size in both series. It can be seen that the geometries change little with increasing chain length (within 0.01 Å). It suggests that the polymerization has little effect on the geometrical structures of repeating unit Ge–TFT or Pt–Ge–TFT.

3.2. Electronic structure

Since the observed differences in the chemical and physical properties of the complexes rely primarily on the changes in the ground-state electronic structure, we will discuss in detail the ground-state electronic structure of these complexes with a special emphasis on the frontier orbital components and HOMO–LUMO energy gaps. Table 3 only shows the most important occupied and virtual (unoccupied) orbitals of $(Pt-Ge-TFT)_1$ as an example. Each molecule is divided into eight parts: the Pt metal, two ethynyl units on the left of the Ge atom (the one close to Pt labeled as C≡C; the one close to the Ge atom labeled as $C{\equiv}C_{Ge}$), 9,9-dimethylfluorenes on the left of the Ge atom (F), $GeMe_2$ group, two ethynyl units on the right of the Ge atom (the one close to Ge atom labeled as $C{\equiv}C_{Ge}{}'$; the one far away from the Ge atom labeled as C≡C′) and 9,9-dimethylfluorenes on the right of the Ge atom (F′). The electron density contours of the characteristic occupied and virtual orbitals for $(Pt-Ge-TFT)_1$, as well as $(Pt-Ge-TFT)_1$ are depicted in Fig. 3 in order to compare and investigate the role of Ge linker and the effects of the Pt metal incorporation on the whole molecule.

In $(Ge-TFT)_1$, as shown in Fig. 3, all the orbitals spread over the whole π-conjugated backbone and the characters between the HOMO and HOMO − 1 and that between the LUMO and LUMO + 1 are very similar. There is antibonding between the bridge atoms of inter-ring and there is bonding between the bridge carbon atom and its adjacent atoms of intra-ring in the HOMO. On the contrary, there are bonding in the bridge single bond of inter-ring and antibonding between the bridge atom and its neighbour of intra-ring in the LUMO. Apparently, the triple bond and fluorene units are able to extend π-conjugation effectively while the $GeMe_2$ group exhibits a partial conjugation effect along the molecular backbone since the two organic segments are separated by Ge–C single bonds.

However, the presence of Pt metal center changes the overall charge distributions. It can be seen that unlike the electron distribution in $(Ge-TFT)_1$, the frontier occupied MOs (*n*HOMOs) in $(Pt-Ge-TFT)_1$ concentrate mainly on the fluorene ring or alkynyl fragment on only one side of the Ge atom, admixed with some contributions from the metal center. In $(Ge-TFT)_1$, the interaction between the p_z orbital of Ge and the two acetylene p_z orbital on both sides of Ge forming two stable Ge–C σ bonds was found, and thus the electron cloud can transfer from one side to another across the Ge atom. On the contrary, only one Ge–C σ bond was found on the left side of Ge atom, whereas the right acetylene is mainly delocalized on p_x and p_y orbitals. So, from here the conjugation was broken. We can find the reasons from the analysis of the frontier orbitals. The weak pπ–dπ interactions between the ligand (p_z) and the metal ($d_{x^2-y^2}$) result in weak delocalization along the molecular chain. The first occupied orbital in $(Pt-Ge-TFT)_1$ consists mainly of π orbitals of the conjugate organic structural unit –[C≡C–F–C≡C]– (∼94%) and also mix slightly with the metal d orbitals (∼6%), followed by one orbital containing completely –[C≡C–F–C≡C]– ligand fragment. On the contrary, improved contribution from the metal $d_{x^2-y^2}$ orbital in an antibonding fashion can be found in HOMO − 2. But it will not participate in the low-lying optical excitation due to their relatively low-energy level. In contrast, the two lowest unoccupied orbitals LUMO and LUMO + 1 in each complex are essentially π* orbitals localized on the –[C≡C–F–C≡C]– moieties (over 98%) and LUMO + 1 is calculated to have less contribution from Ge atom (∼2%). From such analysis, intra-ligand excitation (IL) accompanied

Table 3
B3LYP/E60 calculated one electron energy and percentage composition of selected frontier MOs of $(Pt-Ge-TFT)_1$, expressed in terms of composing fragments

MO	Composition (%)								
L + 1			π*p_z (C≡C) (5%)	+	π*p_z (F) (82%)	+	π*p_z ($C{\equiv}C_{Ge}$) (10%)	+	p_z (Ge) (2%)
L			π*p_z ($C{\equiv}C_{Ge}{}'$) (8%)	+	π*p_z (F′) (82%)	+	π*p_z (C≡C′) (10%)	+	
H	d + 2(Hg) (6%)	+	πp_y (C≡C) (24%)	+	πp_y (F) (62%)	+	πp_y ($C{\equiv}C_{Ge}$) (7%)	+	
H − 1			πp_z ($C{\equiv}C_{Ge}{}'$) (15%)	+	πp_z (F′) (74%)	+	πp_z (C≡C′) (11%)	+	
H − 2	d + 2(Hg) (40%)	+	π (C≡C) (49%)	+	p_y (F) (11%)	+		+	

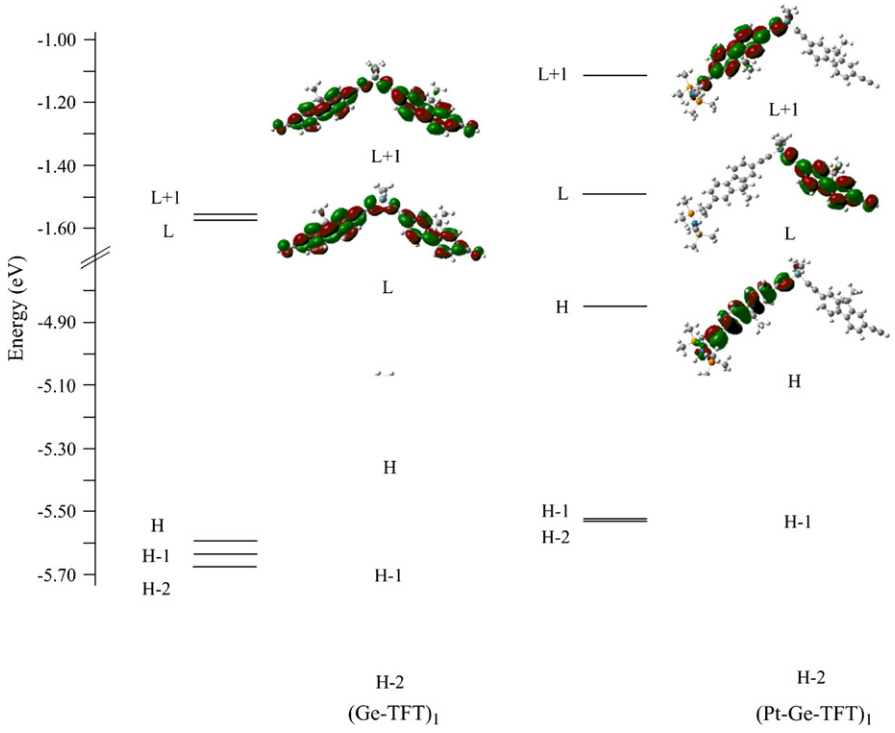

Fig. 3. Energy level diagram of frontier molecular orbitals together with the representative three-dimensional MOs plots calculated at the B3LYP/E60 level for $(Ge-TFT)_1$ (on the left) and $(Pt-Ge-TFT)_1$ (on the right).

by little metal-to-ligand charge transfer (MLCT) was expected during photoexcitation.

To gain a greater insight into this weak delocalization and the evolution from monomer to oligomers, it is worthwhile to compare the energy levels of $(Ge-TFT)_n$ and $(Pt-Ge-TFT)_n$ ($n = 1-3$). The energy levels of HOMO and LUMO of the oligomers in $(Ge-TFT)_n$ and $(Pt-Ge-TFT)_n$ ($n = 1-3$) calculated by B3LYP/E60 are tabulated in Table 4. From Table 4 it can be seen that as is usual in π-conjugated systems, the energy level of the frontier electronic orbitals evolves linearly with inverse chain length in the sp^3-Ge-linked Pt(II) system, as well as in their free ligand system, and with increasing conjugation lengths, the HOMO energies increase, whereas the LUMO energies decrease in both series. The introduction of Pt(II) center lowers significantly the HOMO of the longest oligomer of $(Pt-Ge-TFT)_n$ system by some 0.7 eV, which should thus ensure the efficient hole injection and low charge trapping in optoelectronic devices. Turning to the evolution of the LUMO levels, we find that the LUMOs of the longest oligomer of $(Pt-Ge-TFT)_n$ are destabilized by about 0.1 eV with respect to its free ligand. This slight increase of the LUMO levels would not worsen the electron injection ability.

Table 4
The negative of HOMO and LUMO energies ($-\varepsilon_{HOMO}$, $-\varepsilon_{LUMO}$) (eV) of $(Ge-TFT)_n$ and $(Pt-Ge-TFT)_n$ obtained by B3LYP/E60

Oligomers $(Ge-TFT)_n$	$-\varepsilon_{HOMO}$	$-\varepsilon_{LUMO}$	Oligomers $(Pt-Ge-TFT)_n$	$-\varepsilon_{HOMO}$	$-\varepsilon_{LUMO}$
$n=1$	5.59	1.57	$n=1$	4.85	1.49
$n=2$	5.58	1.56	$n=2$	4.82	1.53
$n=3$	5.55	1.61	$n=3$	4.84	1.51

The results of Table 4 can be easily rationalized by analyzing how the nature of the frontier electronic levels of the free ligand chains is affected by the incorporation of transition metal (see Fig. 4). In Pt–Ge–TFT, the HOMO remains localized along the left TFT conjugated backbone and Pt(II) metal; the shapes of the LUMOs become drastically different, being localized on the right TFT conjugated backbone and none on Pt.

This is rationalized by the fact that the energy separation between the LUMO of $Pt(PMe_3)_2$ and TFT moieties is large (1.37 eV) and leads to weak interactions between the two building blocks; in contrast, the separation between the corresponding HOMO level is smaller (0.14 eV) and promotes stronger interactions between the two units. It is also the reason why the LUMO levels of Pt–Ge–TFT are close to that of Ge–TFT. The strong localization of the HOMO and LUMO levels in Ge-linked Pt(II)-containing copolymer is expected to reduce significantly the interachain mobilities for electrons.

Another important characteristic of the electronic structure induced by the presence of Pt center that we are interested in is the energy gap. Density functional theory (DFT) calculations are employed to obtain HOMO–LUMO gaps of oligomers. The TDDFT is also employed to get the energy gap from the calculated first dipole-allowed excitation energy of their oligomers (as shown in Table 5). The calculated energy gap decreases by about 0.6 eV from the free ligand $(Ge-TFT)_n$ relative to the complex $(Pt-Ge-TFT)_n$, and metal fragment affects the HOMO more than the LUMO. This can be explained by weak delocalization through the metal center and

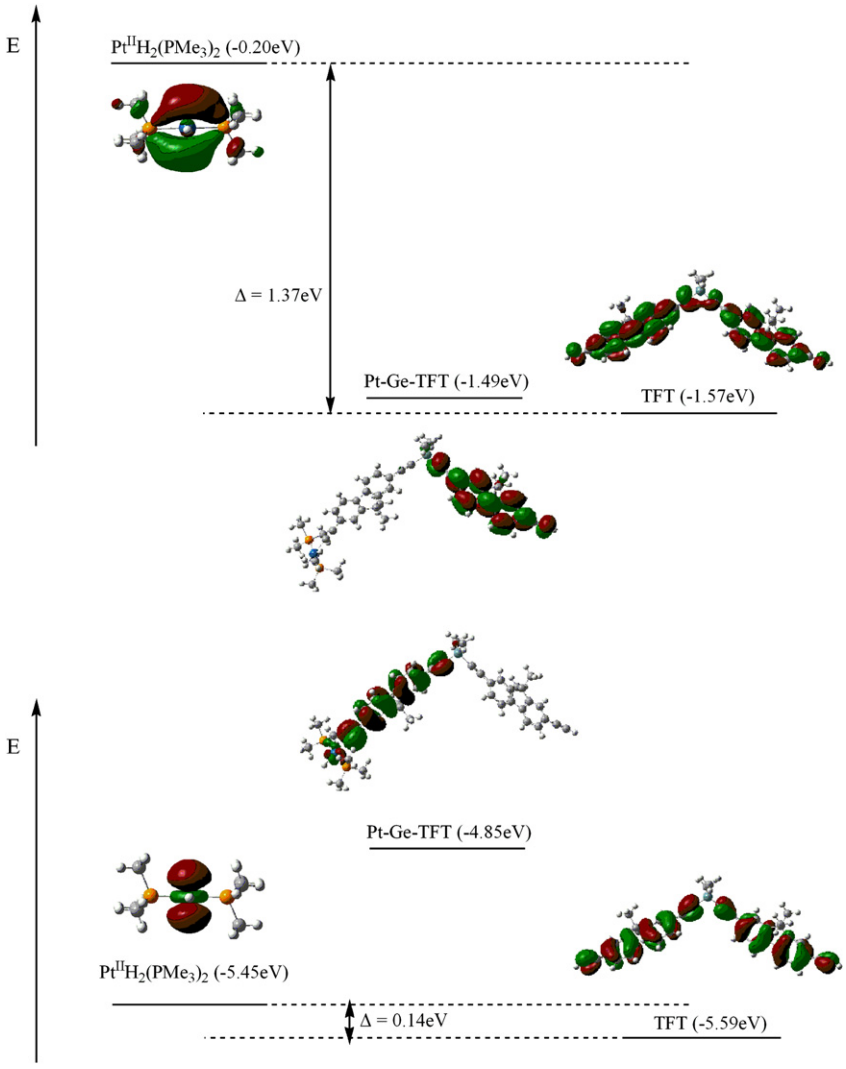

Fig. 4. Energies and shapes of the HOMO (top) and LUMO (bottom) orbitals of $PtH_2(PMe_3)_2$, TFT and Pt–Ge–TFT, as calculated at B3LYP/E60 level.

ligand Ge–TFT. The reduction in the HOMO–LUMO gap observed when going from the free ligand to Pt-containing oligomers will influence the optical properties of the chains.

3.3. Absorption spectra

The TDDFT/B3LYP/E60 has been used on the basis of the optimized geometry to obtain the nature and the energy of the singlet–singlet electronic transitions of all the oligomers in all series under study as reported in Table 6.

Table 5
The HOMO–LUMO gaps (Δ_{H-L}) (eV) by B3LYP and the lowest excitation energies (E_g) (eV) by TDDFT of $(Ge–FTF)_n$ and $(Pt–Ge–FTF)_n$ ($n = 1–3$)

Oligomer $(Ge–FTF)_n$	Δ_{H-L}	E_g (TD)	Expt[a]	Oligomer $(Pt–Ge–FTF)_n$	Δ_{H-L}	E_g (TD)
$n = 1$	4.02	3.81	3.57	$n = 1$	3.36	3.14
$n = 2$	4.02	3.77	3.51	$n = 2$	3.29	3.21
$n = 3$	3.94	3.74	3.49	$n = 3$	3.33	3.18

[a] Optical band gap derived from the absorption edge of a polymer thin film in Ref. [7].

For $(Ge–TFT)_n$ ($n = 1–3$), the low-energy and maximum absorption peaks correspond to π–π* excitation. On the other hand, for $(Pt–Ge–TFT)_n$ ($n = 1–3$), the low-energy absorption band is assigned to π–π* excitation and the maximum absorption peak arises from MLCT excitation. The absorption wavelength increases progressively with increasing conjugation length. The maximum absorption peaks in $(Pt–Ge–TFT)_n$ exhibit bathochromic shifts compared to $(Ge–TFT)_n$ due to the introduction of Pt metal.

4. Conclusions

In this work, the geometrical and electronic structures of $(Pt–Ge–TFT)_n$ and $(Ge–TFT)_n$ ($n = 1–3$) are investigated by DFT and TDDFT methods. π-Conjugation was prevented through the Pt metal atom due to weak hybridization between the pπ-orbital of the conjugated ligand and the Pt dπ-orbital. Further electronic spectrum calculations confirm that the introduction of metal center into the conjugated segments contributes more to confine the electrons than to delocalization of

Table 6
Electronic transition data obtained by the TDDFT/B3LYP/E60 for $(Ge-FTF)_n$ and $(Pt-Ge-FTF)_n$ ($n = 1-3$)

Oligomers	State	Composition	(%)	ΔE (eV)/λ (nm)	f	Expt (nm)	Character
$(Ge-TFT)_1$	S_1	H→L	60	3.81/325.67	0.2351	339	IL
	S_3	H − 1→L + 1	56	3.95/313.54	2.2799		IL
		H→L	28				
	S_4	H − 1→L	47	4.12/300.88	0.5956		IL
		H→L + 1	39				
$(Ge-TFT)_2$	S_1	H→L	45	3.77/328.86	0.4946	343	IL
		H→L + 2	34				
	S_3	H − 1→L	59	3.79/326.64	0.0350		IL
		H − 2→L	32				
	S_4	H − 2→L	45	3.85/321.91	2.2629		IL
		H→L	30				
$(Ge-TFT)_3$	S_1	H→L + 1	60	3.74/331.88	0.2375	345	IL
	S_3	H − 1→L	54	3.76/329.72	0.4474		IL
		H − 2→L + 1	27				
	S_7	H − 3→L	41	3.83/323.52	1.3279		IL
		H − 2→L + 1	30				
$(Pt-Ge-TFT)_1$	S_1	H→L	71	3.14/395.10	0.0008		IL
	S_2	H − 1→L	64	3.50/354.05	1.6967		IL
	S_6	H − 2→L	62	3.91/316.77	1.2417		MLCT
$(Pt-Ge-TFT)_2$	S_1	H→L	62	3.21/386.10	0.0005		IL
	S_3	H→L + 1	59	3.41/362.86	0.2094		IL
		H→L + 2	45				
	S_5	H − 1→L + 1	64	3.44/360.47	1.3972		IL
$(Pt-Ge-TFT)_3$	S_1	H − 2→L	68	3.18/389.73	0.0014		MLCT
	S_4	H→L + 2	66	3.40/364.82	0.1266		IL
	S_5	H − 1→L + 2	46	3.41/363.77	1.7064		IL
		H − 2→L + 1	46				MLCT

the π electrons. The heavy metal atom forms some barrier to delocalization, so that the singlet excited states of oligomers have the character of molecular excited states and mainly the ligand-dominating excited state. Thus this kind of rigid-rod organometallic polymer can be used as a good emitter layer in displays due to their potential in achieving full color emission through modifying the electronic structure of the conjugated ligand segment.

Acknowledgments

This work was supported by the Major State Basis Research Development Program (no. 2002CB 613406) and a CERG grant from the Hong Kong Research Grants Council (no. HKBU2022/03P).

References

[1] Burroughes JH, Bradley DD, Brown AR, Marks RN, Mackay K, Friend RH, et al. Nature 1990;347:539.
[2] Tessler N, Denton GJ, Friend RH. Nature 1996;382:695.
[3] Halls JJM, Walsh CA, Greenham NC, Marseglia EA, Friend RH, Moratti SC, et al. Nature 1995;376:498.
[4] (a) Wong W-Y, Ho C-L. Coord Chem Rev 2006;250:2627;
(b) Wong W-Y. J Inorg Organomet Polym Mater 2005;15:197;
(c) Wong W-Y, Ho C-L. In: Abd-El-Aziz AS, Manners I, editors. Frontiers in transition metal-containing polymers. Wiley-VCH; 2007 [chapter 6].
[5] Wittmann HF, Friend RH, Khan MS, Lewis J. J Chem Phys 1994;101:2693.
[6] (a) Mitschke U, Bäuerle P. J Mater Chem 2000;10:1471;
(b) Kraft A, Grimsdale ACG, Holmes AB. Angew Chem Int Ed 1998;37:402;
(c) Lu JP, Tao Y, D'Iorio M, Li YN, Ding JF, Day M. Macromolecules 2004;37:2442.
[7] Wong W-Y, Poon S-Y, Lee Albert W-M, Shi J-X, Cheah K-W. Chem Commun 2004;2420.
[8] Frisch MJ, Trucks GW, Schlegel HB, Scuseria GE, Robb MA, Cheeseman JR, et al. Gaussian 03, Revision B.04. Pittsburgh, PA: Gaussian, Inc; 2003.
[9] (a) Casida MK, Jamorski C, Casida KC, Salahub DR. J Chem Phys 1998;108:4439;
(b) Stratmann RE, Scuseria GE. J Chem Phys 1998;109:8218.
[10] (a) Monat JE, Rodriguez JH, McCusker JK. J Phys Chem A 2002;106:7399;
(b) Rodrigues JH, Wheeler DE, McCusker JK. J Am Chem Soc 1998;120:12051;
(c) Zheng K, Wang J, Peng W, Liu X, Yun F. J Phys Chem A 2001;105:10899.
[11] (a) Foresman JB, Head-Gordon M, Pople JA. J Phys Chem 1992;96:135;
(b) Belletête M, Beaypré S, Bouchard J, Blondin P, Leclerc M, Durocher G. J Phys Chem B 2000;104:9118.